International Journal of Nanoelectronics and Materials
Volume 14, No. 3, July 2021 [237-246]

The Thermal, Surface Chemical, and Electrical Properties of $BiFe_{1-x}Zn_xO_3$ (x = 0, 0.06, 0.12) Nanocrystalline through Sol-gel Technique

Suharno[1*], B. Soegiyono[2], Sarwanto[1], S. Budiawanti[1], Y. Arimurti[1], D.T. Raharjo[1]

[1]Department of Physics Education, Faculty of Teacher Training and Education,
Universitas Sebelas Maret, Surakarta 57126, Indonesia
[2]Department of Physics, Faculty of Mathematics and Natural Science,
Universitas Indonesia, Depok 16424, Indonesia

Received 6 January 2021, Revised 21 April 2021, Accepted 30 April 2021

ABSTRACT

The synthesis of zinc doped bismuth ferrite has been successfully carried out using the sol-gel autocombustion method. The thermal properties through the TGA test showed that the mass began to stabilize in the range of temperature 600 - 750°C as the indication of the formation of single-phase $BiFe_{0.88}Zn_{0.12}O_3$ nanocrystalline. It is obtained from the SEM test that the surface shape of $BiFeO_3$ of zinc doping indicated that it was not homogeneous and there was clotting. Through the EDS test, it is shown the ratio of (% wt) Bi : Fe between calculations and experiments of 1:1 which indicates a stoichiometric reaction. The XPS study found Zn2p element has entered the Fe2p element. The electrical properties through the LCR test showed that the existence of Zn doped $BiFeO_3$ nanocrystalline reduces the dielectric constant value at a frequency of 100 kHz - 1 MHz. The dielectric constant values are stable at high frequency which can potentially be applied to electromagnetic waves.

Keywords: bismuth ferrite, sol-gel, sintering, homogeneous, dielectric constant

1. INTRODUCTION

The multiferroic material is a material that shows ferroic properties which implied that it can be both ferroelectric and ferromagnetic. The carrier for ferroelectric properties is bismuth oxide (Bi_2O_3) while the carrier for ferromagnetic properties is ferrite (Fe_2O_3). Multiferroic materials can be grouped into single-phase compounds and composites. Bismuth ferrite ($BiFeO_3$) is one of the multi-ferrous material in the perovskite form of ABO_3. Perovskite is a material with the ABX_3 shape. Perovskite material has a cubic structure with Pm-3m symmetry. The cubic symmetry is easy to distort due to the ionized structure of various elements. The crystal structures results from the distortion of the cubic structure are tetragonal, orthorhombic, monoclinic, and rhombohedral. The perovskite structure is strong and able to rotate the bond angles to accommodate a variety of cations. In general, perovskite is a metal oxide with the general formula of ABO_3 where A is the block metal ions of s, d or f while B is the transition metal ions so that the total charge of ions A and B is +6 in order to maintain the balance of the oxygen charge, which amounts to -6 carried by the three oxygen ions.

The $BiFeO_3$ material properties can change through doping on Bi and Fe materials. The choice of doping material for the $BiFeO_3$ multiferroic material was intended as an engineering effort to have

*Corresponding Author: suharno_71@staff.uns.ac.id

better properties and to be suited with the application of the material. The element to be doped at the Bi site should be an ions with charge 3+ such as such as Nd and Y or ions with charge 2+ such as Ca and Zn [1,2]. It was also reported that the $BiFeO_3$ can be doped at Fe site with transition metal such as Zn, Cu, and Mn [3,4]. The synthesis of $BiFeO_3$ material can be made through the solid-state reaction and sol-gel techniques. The synthesis using sol-gel technique requires the basic ingredients of bismuth nitrate, iron nitrate and citric acid was added to obtained plus as ingredients to produced gel [5,6]. Research on thermal properties reported that the TGA test for $BiFeO_3$ material which synthesized through the sol-gel method with addition tartaric acid as fuel, the mass drop occurred at temperatures of 150˚C [7]. Research on electrical properties reported that the effect of Sm, La, and Mn doped $BiFeO_3$ can reduce the dielectric constant value [8,9,10].

The synthesis of bismuth ferrite with sol-gel technique is reported in this article. The heated of samples were carried out to obtain bismuth ferrite nanocrystals. The application of zinc doped bismuth ferrite expected to change the thermal, microstructurital, and electrical properties of bismuth ferrite.

2. MATERIAL AND METHODS

In this experiment, zinc doped bismuth ferrite synthesized with sol-gel autocombustion technique and using the basic ingredients of $Bi(NO_3)_3.5H_2O$, $Fe(NO_3)_3.9H_2O$, $Zn(NO_3)_2.6H_2O$, and citric acid ($C_6H_8O_7$) as fuel.

The basic ingredients were mixed stochiometrically with concentration of 0.2 M on all the basic ingredients and the mole ratio of bismuth nitrate, iron nitrate, citric acid solution were 1 : 1 : 1.67. Furthermore, the solution mixture were stirred in a glass with a magnetic stirrer on the hotplate for 3 hours with a hot plate temperature of 260°C until gel was obtained. The addition of citric acid to the mixture serves as a solution in synthesis. After the gel was obtained, it was dried at a temperature of 150°C for 1 hour. The zinc doped bismuth ferrite nanoparticles were obtained after grounding and heating at a temperature of 750°C for 5 hours. Finally, the samples were crushed for several hours so that it were homogeneous and there were no clumping of particles. The samples obtained in this study were $BiFe_{1-x}Zn_xO_3$ (x = 0, 0.06, 0.12).

The thermal properties of the samples were measured with a Thermogravimetric Analysis STA 6000 PerkinElmer at a temperature range of 30 - 800°C with a heated rate of 10°C.min^{-1} and Argon gas flow of 20 mL.min^{-1}. The surface shape of the samples were measured with the FE-SEM brand FEI INSPECT type F50. The binding energy of the samples were measured at a spectrum of 0 - 800 eV. The electrical properties of the samples were measured with LCR meter type HIOKI 3532-50 at a frequency of 40 Hz - 1 MHz.

3. RESULTS AND DISCUSSION

3.1. The Thermal Analysis

The thermal analysis was carried out on zinc doped bismuth ferrite with concentrations (wt%) at 6% and 12% after the formation of the gel and dried to 150°C. This analysis was conducted to find out the change in mass towards the temperature in the $BiFe_{1-x}Zn_xO_3$ phase formation process (x = 0, 0.06, 0.12). TGA thermal test is as shown in Figure 1.

Measurements were made in a temperature range of 30 - 800°C, heated speed of 10°C/minute, and Argon gas flow of 20 mL/minute. The results of the TGA thermal test in the temperature range of 150 - 750°C obtained shows changes in mass of the material as shown in Table 1.

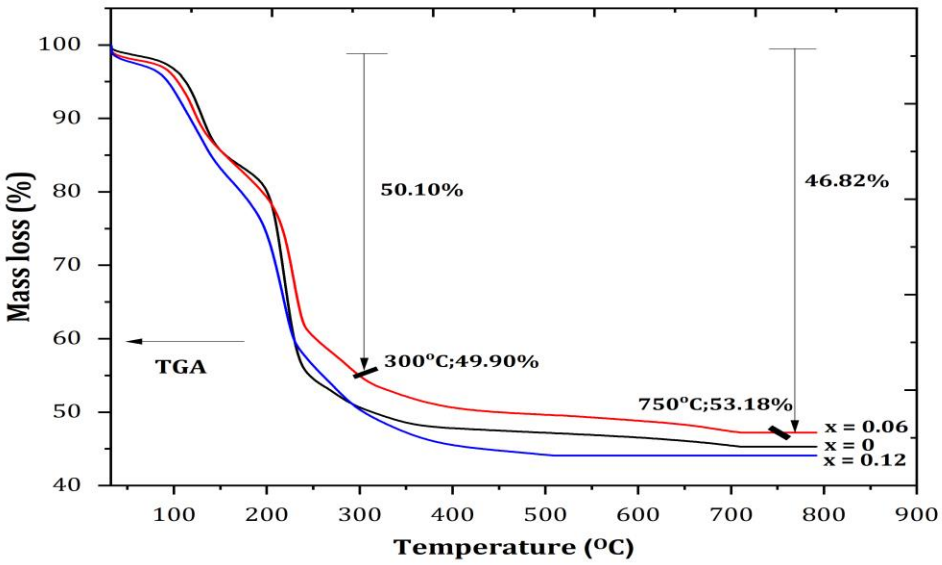

Figure 1. TGA of $BiFe_{1-x}Zn_xO_3$ (x = 0, 0.06, 0.12) nanocrystalline

From this table, it is shown that in the temperature range of 150 - 300°C in $BiFe_{0.88}Zn_{0.12}O_3$, there was a decrease in mass significant in the amount of 1.2802 mg due to the very large evaporation of water, which shows mass changes. In this condition, it indicates the occurrence of autocombustion and exothermic reactions in the sample. The other conditions in the temperature range of 300 - 450°C show that there was a very slight mass decrease of 0.1888 mg so that it was indicated as the beginning of the formation process of $BiFe_{0.88}Zn_{0.12}O_3$. The temperature range of 450 - 600°C shows a small decrease in mass, namely 1.1044 mg. In the temperature range 600- 750°C, it shows that the mass loss was starting to stablised. This condition indicates that the formation of the $BiFe_{0.88}Zn_{0.12}O_3$ phase was getting better.

Table 1 Mass decrease of $BiFe_{1-x}Zn_xO_3$ (x = 0, 0.06, 0.12) nanocrystalline with TGA Analysis

Temperature (°C)	x = 0		x = 0.06		0.12	
	Mass (mg)	Mass loss (%)	Mass (mg)	Mass loss (%)	Mass (mg)	Mass loss (%)
150	7.4752	84.51	7.4402	84.16	7.4028	83.62
300	5.0607	50.10	5.7590	54.81	5.0604	50.08
450	3.6622	47.47	3.7601	50.15	3.5637	44.63
600	3.5098	46.56	3.6957	48.97	3.3517	43.97
750	3.4875	44.38	3.5743	46.82	3.0878	43.76

Based on the TGA thermal test, the synthesis of samples was carried out through sintering at 750°C for 5 hours and to obtain a more dominant single-phase $BiFeO_3$. The sintering time at 750°C will affect the particle size distribution.

3.2. The Composition and Microstructure

The $BiFeO_3$ and zinc doped $BiFeO_3$ elements have a composition of Bi, Fe, Zn, O, and C as shown in Table 2. The EDS test results as shown in Table 2 have the percentage of weight fraction (wt%) of the composition of Bi, Fe, and O in $BiFeO_3$, $BiFe_{0.94}Zn_{0.06}O_3$, and $BiFe_{0.88}Zn_{0.12}O_3$.

This result shows the ratio (%wt) of Bi:Fe between calculation and experiment was closed to 1:1 which indicates a stoichiometric reaction. Figure 2 shows the EDS spectrum of the $BiFeO_3$ material composition. It is also observed that in $BiFeO_3$ synthesis, a carbon atom appears at the end, this is because $BiFeO_3$ has the nature of a carbon residue or easily absorbs carbon.

(a)

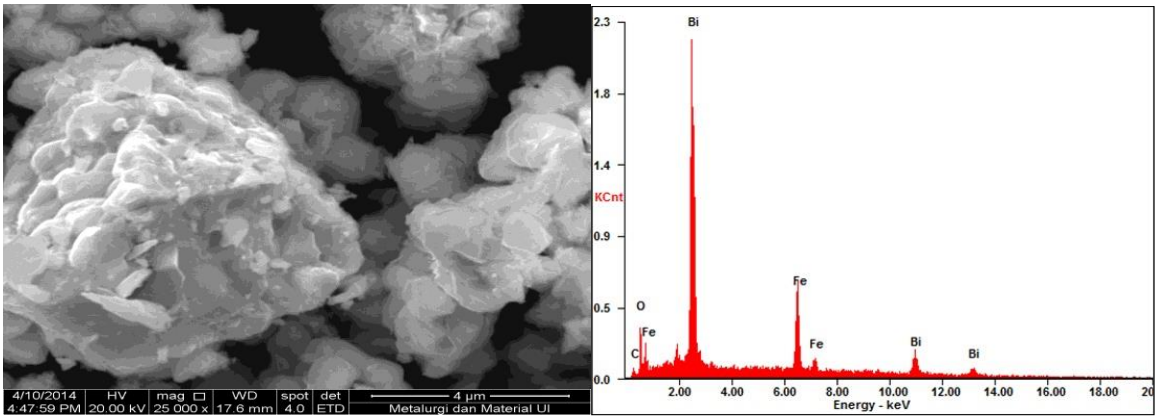

(b)

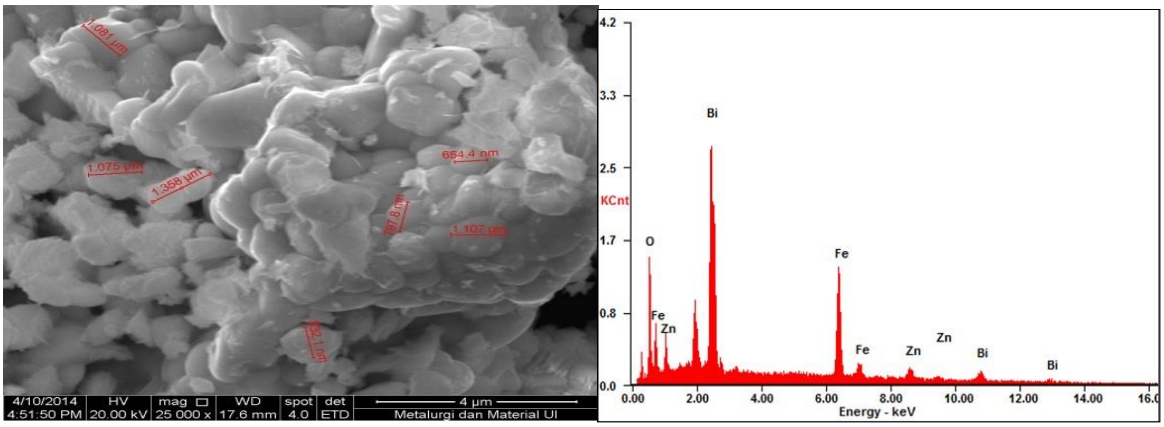

(c)

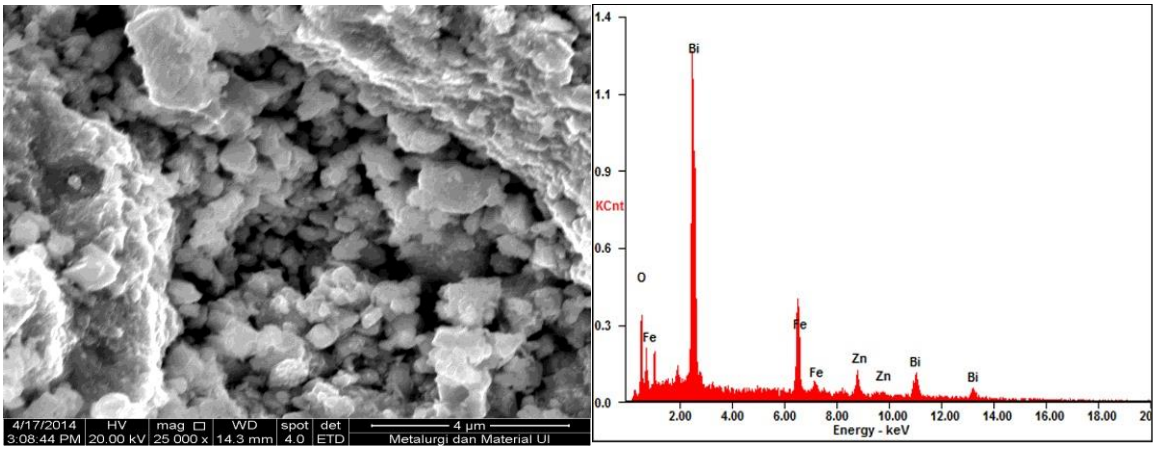

Figure 2. The microstructure and EDS spectrum of $BiFe_{1-x}Zn_xO_3$, nanocrystalline (a) x = 0, (b) x = 0.06, (c) x = 0.12

Table 2 The composition weight fraction of $BiFe_{1-x}Zn_xO_3$, (x = 0, 0.06, 0.12)

Element	Weight fraction (% wt)		
	x = 0	x = 0.06	x = 0.12
Bi	67.32	58.67	60.76
Fe	17.49	16.74	14.13
Zn	0.00	6.40	10.20
O	14.04	18.20	14.91
C	1.14	0.00	0.00

The results of SEM photos show the shape and size of the particles of $BiFe_{1-x}Zn_xO_3$, (x = 0, 0.06, 0.12) as shown in Figure 2 and the average particle size of $BiFe_{1-x}Zn_xO_3$, (x = 0, 0.06, 0.12) are 447 nm, 407 nm, and 339 nm. These results were the same as in the previous studies that through SEM studies, the surface shape of the particles shows clumping and they are not homogeneous, as in previous studies [5,11].

It can be concluded that the surface shape of the zinc doped $BiFeO_3$ particles shows an indication of not being homogeneous and clotting occurred, causing decrease in the average size of the particles.

3.3. The X-Ray Photoelectron Spectroscopy (XPS) Study

The binding energy elements Bi, Fe, O were studied using XPS at a spectrum interval of 0 - 800 eV as shown in Figure 3(a). The determination of the element $BiFeO_3$ with XPS using the concept of the atomic spectrum. The electron state of an atom was related to the principal quantum number, orbital angular momentum, spin angular momentum, and total angular momentum. In the LS coupling concept, the orbital angular momentum was the sum of the orbital angular momentum and spin angular momentum. When the element was in the $2p_{3/2}$ state it means n = 2, l = 1 (p orbital), and s = $+\frac{1}{2}$, so the value of j = l + s = 1 + ($+\frac{1}{2}$) = 3/2.

In this process, when the sample was shot by a photon, there was a photoelectron at the energy levels Bi4f and Fe2p as shown in Figure 3(b) and 3(c). The kinetic energy of the photoelectrons decreases as the electrons move from one orbital to another which was empty and the result here was a peak related to binding energy. The binding energy of $BiFe_{1-x}Zn_xO_3$ (x = 0, 0.06, 0.12) have orbitals $Bi4f_{7/2}$, $Bi4f_{5/2}$, C1s, $Bi4d_{5/2}$, $Bi4d_{3/2}$, O1s, $Fe2p_{3/2}$, and $Fe2p_{1/2}$ with the binding energy value 282 eV, 439 eV, 465 eV, 526 eV, 677 eV, dan 709 eV (Fig.4a). As a result of Zn doping, there was no visible energy binding peak. The Fe had two emission photo peaks corresponding to $Fe2p_{3/2}$ and $Fe2p_{1/2}$ which indicated the oxidation state of Fe^{3+}[12]. There were three peaks of emission photos around Fe2p which are called pre-peak, surface peak and satellite peak (Fig.3b). The appearance of the C1s peak on $BiFeO_3$ indicates impurity but in small amounts with binding energy at 282 eV. The peak of the emission photo with the binding energy at corresponding to O1s indicated the oxidation state of O^{2-} in $BiFeO_3$. Furthermore, the peak photo emission with binding energy at 439 eV and 465 eV corresponds to the peaks of $Bi4d_{5/2}$ and $Bi4d_{3/2}$. Added, the peaks of $Bi4f_{7/2}$ and $Bi4f_{5/2}$ have energy binding at 158 eV and 164 eV (Fig.3c). The peaks of Bi4d and Bi4f indicate the oxidation state of Bi^{3+} or trivalent oxidation state.

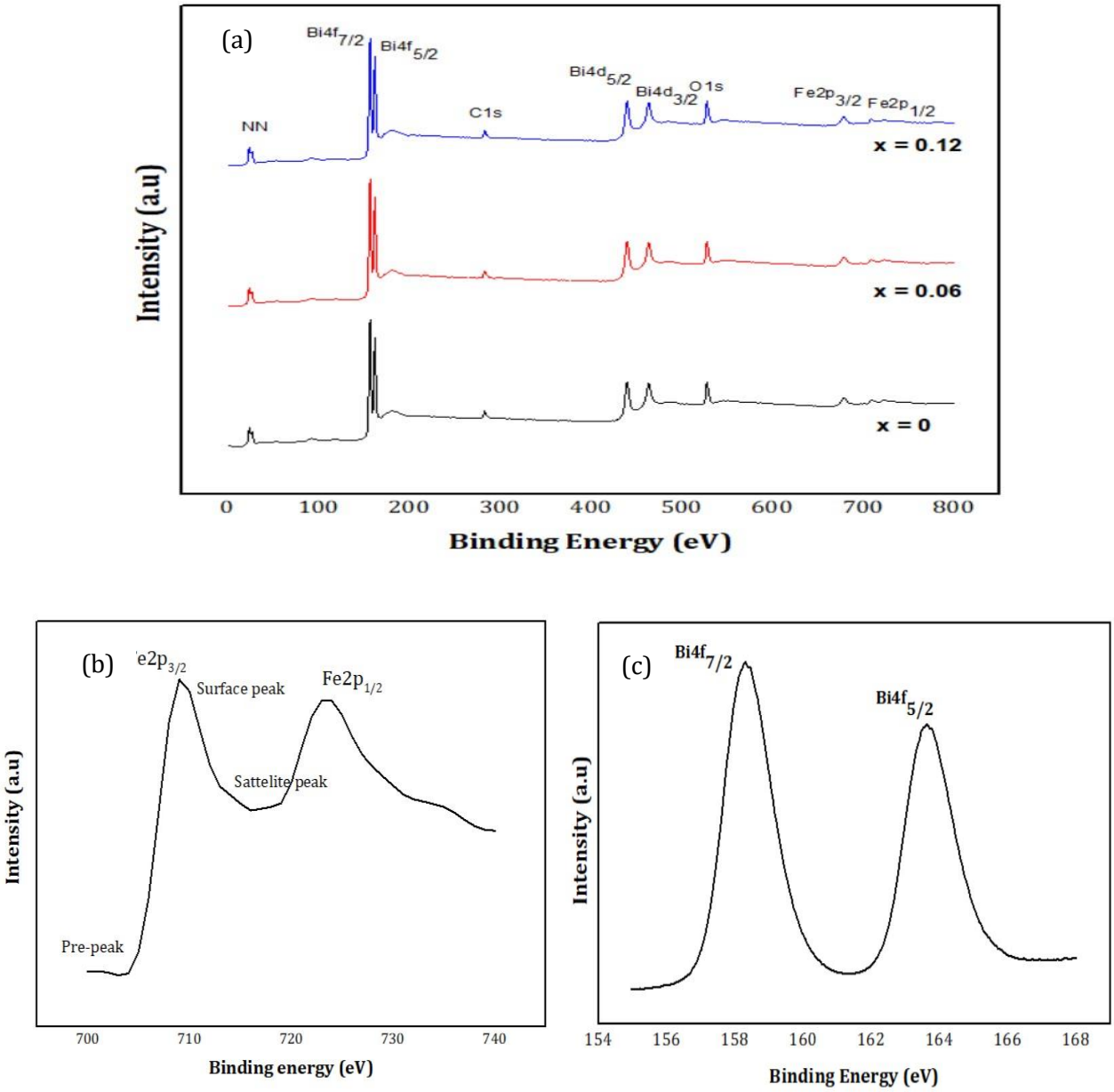

Figure 3. The XPS spectrum analysis of (a) $BiFe_{1-x}Zn_xO_3$ (x = 0, 0.06, 0.12) nanocrystalline, (b) Fe2p, (c) Bi4f

The binding energy of Zn analysis element, had orbital $Zn2p_{3/2}$ and $Zn2p_{1/2}$. This indicates that the Zn2p element has entered the Fe2p element but did not enter the Bi4f element and at other binding energies and the Zinc atom replaces the missing Fe atoms through substitution of Zn^{2+} ions with Fe^{2+}/Fe^{3+} ions. In addition to the Bi, Fe, and O elements, the XPS spectrum of $BiFeO_3$ was also found with C atom. This is because $BiFeO_3$ had a residue of carbon atom in the synthesis process.

3.4. The Electrical Properties

The electrical properties of this material were tested using an LCR meter to find out the value of the dielectric constant. The dielectric constant values of samples were measured against the frequency function. Figure 4 shows that giving Zn substitution can decrease the dielectric constant value and increase of Zn doped $BiFeO_3$ on 6 - 12% (%wt).

Figure 4(b) also shows that at a frequency of 1 MHz, the dielectric constant value of $BiFe_{1-x}Zn_xO_3$ (x = 0, 0.06, and 0.12) is 45, 27, and 35. At this frequency width which was in the high frequency category shows the dielectric constant value tends to be stable so that it has the potential to be applied in the world of industrial technology. Furthermore, Figure 4(a) shows that at a frequency of 1 kHz the dielectric constant values were 351, 239, and 270. The decrease in the doping dielectric constant value of Zn substitution x = 0.06 occurs because of the change in electric polarization with a small volume which affects the decrease in the total electric dipole moment of $BiFeO_3$. This also occurs at the dielectric constant value at low frequencies (50 Hz - 1 kHz) as shown in Figure 5(a). The increase in Zn doping with the substitution of x = 0.06 and 0.12 into Fe were caused by an increase in the electric polarization of Zn^{2+} in a larger volume of $BiFeO_3$ anion which resulted in a decrease of particle size [13]. The increase in the electric dipole moment in the cation also affects the increase in the total electric dipole moment of $BiFeO_3$.

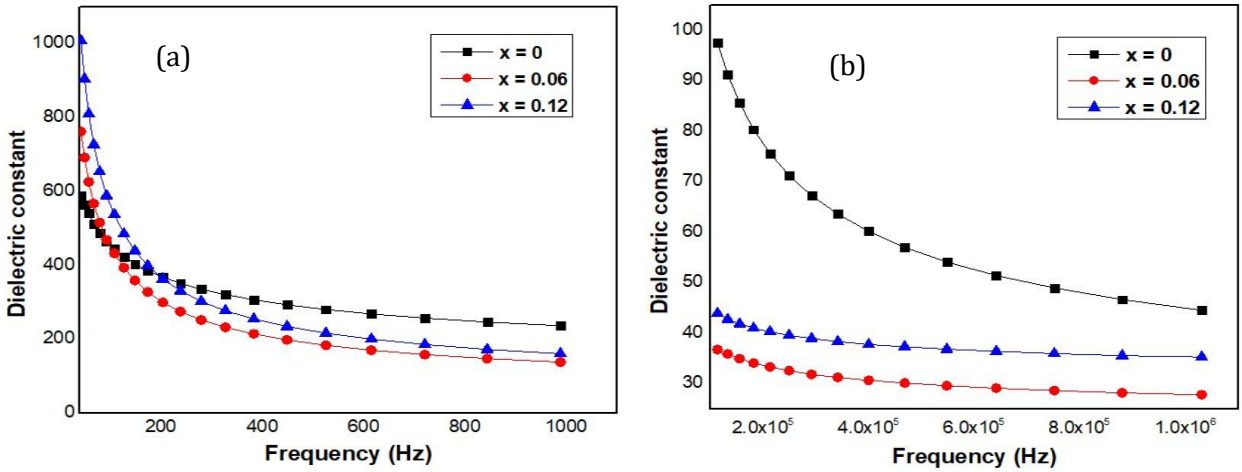

Figure 4. The dielectric constant of $BiFe_{1-x}Zn_xO_3$ (x = 0, 0.06, 0.12) nanocrystalline
(a) Low frequency (50 Hz – 1 kHz), (b) High frequency (100 kHz – 1 MHz)

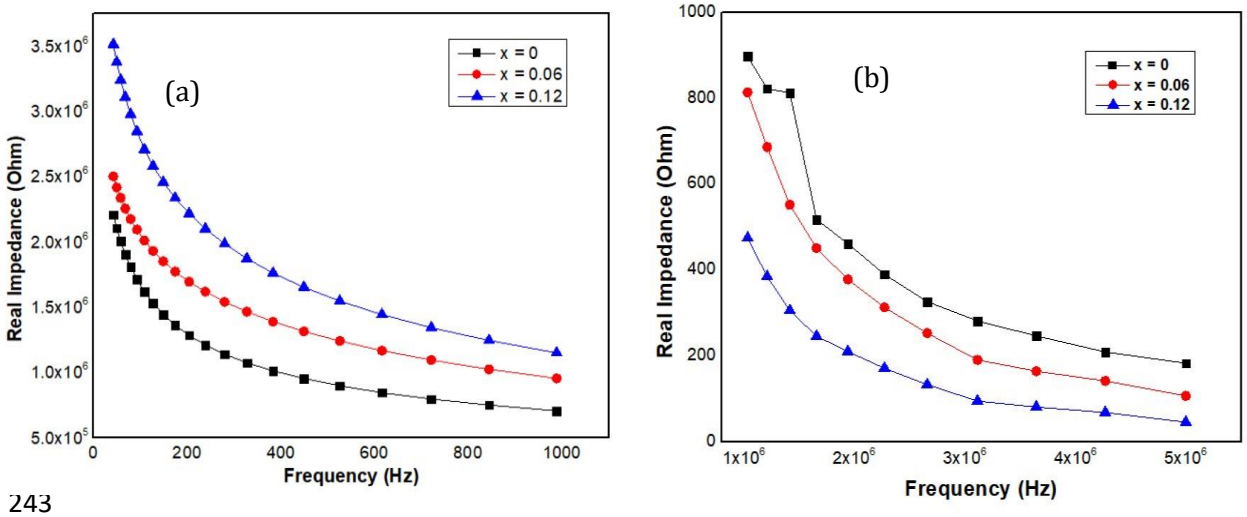

Figure 5. The real impedance of $BiFe_{1-x}Zn_xO_3$ (x = 0, 0.06, 0.12) nanocrystalline (a) Low frequency (50 Hz – 1 kHz), (b) High frequency (1 – 5 MHz)

It can be concluded that the doping of Zn into Fe atom, increases the dielectric constant value of the $BiFe_{0.94}Zn_{0.06}O_3$ material and has potentially to increase the electrical permittivity so that the stored energy was even greater.

Figure 5 shows the real impedance to frequency. Figure 5(a) shows that with Zn doped $BiFeO_3$, there was an increase in the real impedance value, which results in lower electrical properties. However, at high frequencies the opposite occurs, the presence of Zn doping causes a decrease in the real impedance value as shown in Figure 5(b) and this shows that there is an increase in electrical properties and this material is very suitable to be applied to electromagnetic wave sensors.

4. CONCLUSION

The synthesis of zinc doped bismuth ferrite has been successfully prepared using the sol-gel method. At temperatures of 600 - 750°C, there was an indication of the formation of single-phase $BiFeO_3$ nanocrystalline. The surface shape of Zn doped $BiFeO_3$ nanocrystals shows clumping and heterogeneity. Through photoelectron spectroscopy, it did not show any difference in spectral patterns and binding energy due to zinc doped bismuth ferrite. The impact of Zn doped $BiFeO_3$ nanocrystalline have reduced the dielectric constant value at a frequency of 100 kHz - 1 MHz with a stable value at high frequency which could potentially be applied to electromagnetic waves.

ACKNOWLEDGEMENTS

The authors would like to thank LP2M Universitas Sebelas Maret Surakarta for their support in this research through the letter of agreement number 124/UN27.21/HK/2020.

REFERENCES

[1] Hemanta Singh H, Churchill Singh E, Basantakumar Sharma H., Integrated Ferroelectrics. Informa UK Limited, vol **203**, issue 1 (2019) pp. 108–119.
[2] Ma C, Li N, Song W-L., Frontiers in Materials. Frontiers Media SA, vol **7,** (2020) pp. 1-10.
[3] Yang S, Zhang F, Xie X, Sun H, Zhang L, Fan S., Journal of Alloys and Compounds. Elsevier BV, vol **734**, (2018) pp. 243–249.
[4] Yang S, Zhang F, Xie X, Guo X, Zhang L, Fan S., Journal of Materials Science. Springer Science and Business Media LLC, vol **28,** issue 20 (2017) pp. 14944-14948.
[5] Bismibanu A., International Journal for Research in Applied Science and Engineering Technology (IJRASET). vol **6,** issue 4 (2018) pp. 1767–1770.
[6] Abushad M, Khan W, Naseem S, Husain S, Nadeem M, Ansari A. Ceramics International. Elsevier BV, vol **45**, issue 6 (2019) pp. 7437–7445.
[7] Pandey R, Panda C, Kumar P, Kar M., Journal of Sol-Gel Science and Technology. Springer Science and Business Media LLC, vol **85,** issue 1 (2017) pp. 166–177.

[8] Maran R, Yasui S, Eliseev E, Morozovska A, Funakubo H, Takeuchi I, Advanced Electronic Materials. Wiley, vol **2,** issue 8 (2016) p. 1600170.
[9] Musavi Ghahfarokhi SE, Larki MR, Kazeminezhad I., Vacuum. Elsevier BV, vol **173**, (2020) p. 109143.
[10] Rhaman MM, Matin MA, Hakim MA, Islam MF, "Dielectric, ferroelectric and ferromagnetic properties of samarium doped multiferroic bismuth ferrite," Materials Research Express. IOP Publishing, vol **6,** issue 12 (2019) pp. 1250-1280.
[11] Mukherjee S., International Ceramic Review. Springer Science and Business Media LLC, vol **68,** issue 5 (2019) pp. 42–51.
[12] L. F. Goncalves, L. S. R. Rocha, E. Longo, A. Z. Simões, J Mater Sci. Mater Electron, Springer Science and Business Media LLC, vol **29,** issue 1 (2017) pp. 784–793.
[13] Soibam I, Devadatta Mani A., "Optimisation and the Effect of Addition of Extra Bismuth on the Dielectric and Optical Properties of Bismuth Ferrite (BFO)," MaterialsToday Proceedings. Elsevier BV, vol **5,** issue 1 (2018) pp. 2064–2073.